



ICA 2013 Montreal

Montreal, Canada

2 - 7 June 2013

Engineering Acoustics

Session 4pEAa: Sound Field Control in the Ear Canal

4pEAa2. Sound transmission in a simple model of the ear canal and tympanic membrane

Antonio Gonzalez-Herrera, Kapil Wattamwar, Christopher Bergevin and Elizabeth S. Olson*

***Corresponding author's address: OTO/HNS and Biomedical Engineering, Columbia University, New York, NY 10032, eao2004@columbia.edu**

The classic picture of middle ear (ME) transmission has the tympanic membrane (TM) as a rigid piston and the ME space as a vacuum. However, the TM moves in a complex wavy pattern and modern theories link this behavior to the ME's broadband transmission (for example, Fay et al, PNAS 2006; Parent and Allen, 2004). Rabbitt (1990) predicted that the TM transmitted considerable sound pressure into the ME space that could in return affect TM motion. This study explores these ideas with a simple model, using a tube terminated with a plastic "plate." We measured plate motion via laser interferometry, and pressure on both sides via micro-sensors that allowed positioning very close to the plate without disturbance. We made a finite element model of the system to complement the experimental results. The theoretical results show the interaction of acoustic and mechanical resonances, and both theoretical and experimental results show strong transmission of pressure through the membrane at some of its resonant frequencies.

Published by the Acoustical Society of America through the American Institute of Physics

INTRODUCTION

In the mammal, sound pressure at the pinna travels down the ear canal and drives TM motion, leading to ossicular motion and cochlear excitation. TM motion also produces pressure in the ME space. In recent work the TM has been modeled as a wave system, which is a departure from the piston approximation employed in many models. This development was based on both modern measurements of the complex TM motion (Tonndorf and Khanna 1972; Rosowski et al, 2009; de La Rochefoucauld and Olson, 2010) and the recognition that a wavy TM motion overcomes the mass limitation of a piston at high frequencies (Fay et al, 2006). A wave is in essence a resonant system - one that can resonate at many frequencies, since the effective mass and stiffness change with wavelength. Thinking of the TM as a wave system leads to some interesting predictions, because when operating at a resonant frequency the TM would move a lot and this seems likely to produce significant pressure in the ME space. Reflected from the bony surface of the back-wall, this pressure would excite the TM from the back and influence the cross-TM pressure drop, as had been explored in a schematic model of TM/air-space interaction by Rabbitt (1990). In this paper we explore some of these concepts with simple physical + finite element models (FEM). We modeled several related systems with the FEM, and their geometry is as shown to the right of the color plots in Fig. 1. The open-open tube and open-closed tube conditions were useful for confirming that the FEM would predict the standard acoustic resonances (Fig. 1A and B). The baffled system (Fig. 1C) was composed of thin plastic covering a hole in a large sheet and was useful to find the plate's mechanical resonances. Two of the FEM systems were tested with measurements on physical models: The tube terminated on one side with a plate (tube+plate system, Fig. 1D and E) and the baffled plate (Fig. 1C and Fig. 2). A more complete report is in preparation; here we present a subset of the experimental and FEM results.

METHODS

The moving component of both the tube and baffle systems is referred to as a "plate," as described below. The physical tube+plate system was made by lightly stretching saran wrap over the end of a glass tube of inner diameter 5.8 mm and length 43mm. The slight stretch was needed to prevent wrinkles. The thickness of the saran wrap was 0.013 mm. For the baffle experiment, in order to get a wrinkle-free plate instead of saran wrap we used scotch tape, placed to cover a hole of diameter 5.8 mm in a piece of plexiglass. The plexiglass thickness was 2.6 mm and its outer dimension (the extent of the baffle) ~ 20 cm. The tape thickness was ~ 50 μ m. A thin film of gold (~ 50 nm) was evaporated onto the plates to make them reflective for laser-interferometric motion measurements.

Pressure was measured with fiber-optic pressure sensors of outer diameter 125 μ m that were constructed in the lab (Olson, 1998). The velocity of the plate in the direction perpendicular to its surface was measured with a heterodyne interferometer that was coupled to a translation and rotation stage for precision positioning of the sample (Khanna et al, 1996). Stimulus generation and data acquisition were performed with the Tucker Davis Technologies system II and Matlab. For the tube experiments the pressure drive was provided by a Radio Shack tweeter terminated by a speaker-tube. The speaker-tube was positioned ~ 1 cm from the plate at an angle of 45°. For the baffle experiment the sound source was a Sony earbud positioned ~ 2 cm from the plate at a 45° angle. A reference pressure was measured halfway between the sound source and the plate. The sound pressure level was ~ 90dB SPL at the reference. Data analysis was performed with Matlab.

Finite element modeling: The numerical model comprised two domains, the solid corresponding to the plate and the fluid corresponding to the surrounding air. The fluid was limited to the volume within a sphere. The sphere surface was meshed by a specific ANSYS element (FLUID130), which represents a fluid domain that extends to infinity. The tube was a rigid boundary. Sound pressure was applied at an approximate distance of 1 cm and 45° from the plate (see Fig. 1), corresponding to the experimental set up. The fluid was meshed with acoustic elements (FLUID30) assuming a compressible and inviscid fluid with uniform mean density and pressure. The speed of sound was 343 m/s and the air density was 1.21 kg/m³. The acoustic absorption coefficient for the tube surface was 0.003 and for the plate was 0.01; these values were found by fitting model predictions to experimental results. The plate can be described as a "membrane" due to its very small thickness (13 microns) compared with its radius (2.9 mm). However, because of the small displacement amplitude the membrane behaves as a plate, where bending is dominant, and the stresses and motions are linear. Thus the term "plate" was used. Experimentally the plate in the tube system was made of saran wrap, and the mechanical properties of the material were: density 940 kg/m³, Poisson's ratio 0.49 and Young's modulus 250 MPa. Damping was applied as a material damping ratio equal to 0.001 (0.1%). This parameter was estimated initially and then updated based on the experimental results. The plate

was meshed with solid element (SOLID185). Because of the thinness of the plate some numerical problems needed to be addressed. They were solved using an enhanced strain formulation and determining the minimum element size to assure convergence (details of the process will be given in another paper). The plate was meshed with a maximum element size of 130 μm . Close to the plate the fluid mesh size was also 130 μm and gradually increased to a maximum size of 1.7 mm. A small amount of pre-stress was applied to the model plate to reproduce the experimental condition. The amount of pre-stress is difficult to measure or estimate, but at the same time increased the mechanical resonance frequencies of the plate significantly. This parameter was estimated based on the experimental results. The pre-strain was $\epsilon_{11} = 0.00275$, which corresponds to a very small radial stretch, $\sim 8\mu\text{m}$. The pre-stress was needed in order for the model to produce the mechanical resonances accurately but did not change the qualitative results. In this paper the FEM of the baffle plate was like that of the tube plate, thus it was not precisely matched to the experimental baffle conditions.

RESULTS

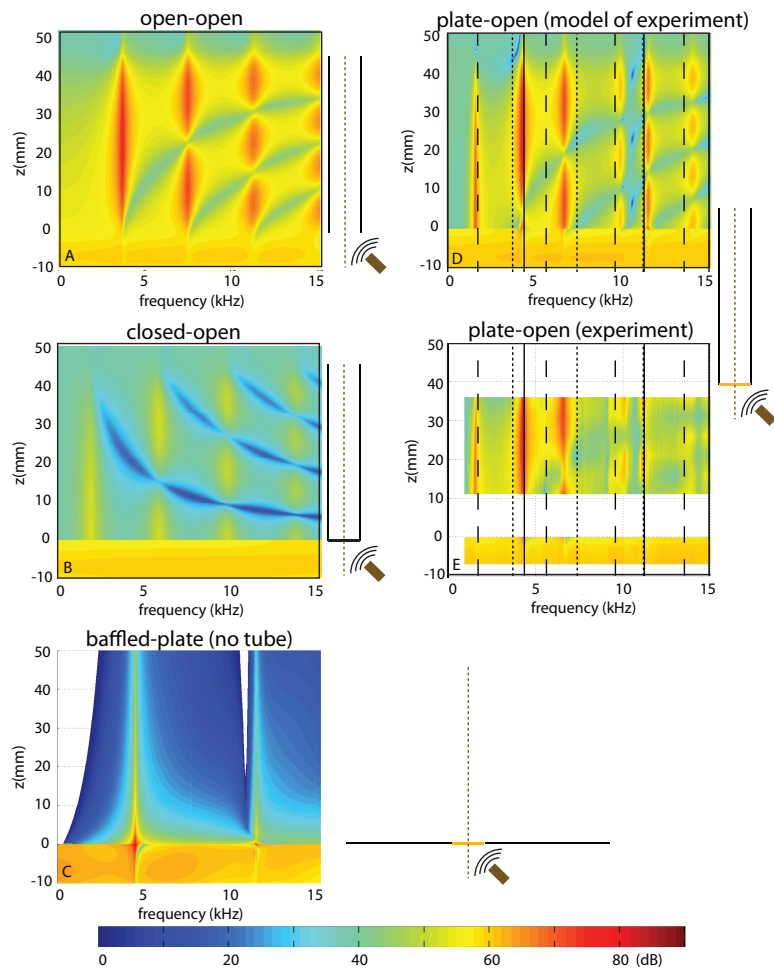


FIGURE 1. A-D FEM pressure results. System geometry is sketched to the right of each color plot. Pressure amplitude is indicated in color as dB relative to a reference location near speaker. Pressure was found on the center-line indicated by the dashed line in the sketches. A. open-open tube. B. closed-open tube. C. baffled plate. D. tube open on far side with plate on side near speaker. E. Experimental results corresponding to D. The pressure was not measured close to the plate within the tube for technical reasons. Vertical lines in D and E were derived from A, B and C as follows: Dashed line = closed-open resonance frequencies from B. Dotted lines = open-open resonances from A. Solid lines = mechanical resonances from C.

Fig. 1 A and B show that the FEM predicted the fundamental acoustic resonances of the open-open (A) and open-closed (B) tubes. Integer half-waves produce the resonances for the open-open case and odd-integer quarter-waves produce the resonances for the open-closed case. With the 43 mm tube length and speed of sound 343 m/s, these corresponded to frequencies of 4, 8, 12, 16 ... kHz for the open-open tube and 2, 6, 10, 14 ... kHz for the open-closed tube. The baffle in C had a mechanical resonance at ~ 4.2 kHz and another at ~ 11.5 kHz. These correspond to the first two circularly symmetric modes of a plate, the first a simple uni-modal motion and the second a “sombbrero” mode in which the center and surround move out of phase. In a vacuum these modes are separated by a factor of 2.3 but due to the mass of the air the lower resonance was reduced in frequency and their separation was slightly larger. (As noted above, Fig.1 presents pressure on the central axis perpendicular to the plate; when off-center pressure is evaluated non-circularly symmetric modes are also predicted by the baffle model.) It is clear, particularly at 4.2 kHz, that at the mechanical resonances the pressure at the plate was increased on both sides due to its motion. For the 4.2 kHz resonance, on the high-frequency side of the resonance the pressure on the speaker side was clearly reduced (blue region at ~ 5 kHz), indicating that the large resonant motion of the plate produced substantial pressure and it was out of phase with the drive pressure at frequencies above the peak, leading to partial cancellation. Experimental verification for these modeling predictions is shown in Fig. 2 and will be discussed below.

The tube+plate FEM prediction in Fig. 1D shows elements of the predictions from the simpler systems in Figs. 1 A, B and C. To help relate it to these simpler systems, vertical lines are drawn to identify the open-open resonances (dotted lines), open-closed resonances (dashed lines) and mechanical resonances (solid lines). The plate is something between an open and a closed condition and the resonances in Fig. 1D are generally different although some nearly overlap with those of the simpler systems. The mechanical resonances happened to lie close to open-open resonances and both are clear in the combined system. The experimental results in Fig. 1E were very similar to the FEM prediction of Fig. 1D, confirming the ability of the FEM to capture the behavior of this system. For example, in both D and E cancellation between drive pressure and pressure caused by the plate motion is apparent in the small region of blue coloring on the high-frequency-side of the resonances at ~ 4.2 and ~ 7 kHz.

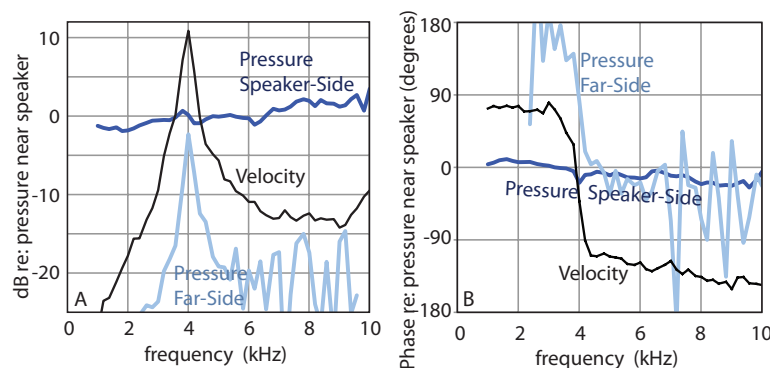


FIGURE 2. Experimental results on the baffle system. Pressure was measured ~ 2 mm from the plate on both the speaker and far side. Velocity was measured at the plate center. A. Amplitude shown as dB relative to the reference pressure measured between the speaker and plate (~ 1 cm from each). B. Phase relative to the reference pressure. The convention for positive velocity direction is into the plate from the speaker-side to far-side.

Experimental results on the baffle system are in Fig. 2. The lowest order resonance occurred at 4 kHz, where both the plate velocity and the pressure on the far side of the plate had a sharp maximum. At the resonance there is only 2 dB pressure drop across the plate, a factor of 0.8. The speaker-side pressure had a small (~ 1 dB) peak on the low-side and small dip on the high-side of the resonance. This was qualitatively similar but smaller than what was predicted in Fig. 1C, and likely the quantitative difference arose because the plate in the experiment was composed of scotch tape, not saran wrap as in the FEM. The far-side pressure appeared noisy above ~ 5.5 kHz. Nevertheless, these data were well above the noise level of the pressure sensor. The noisy-looking pressures might have been produced by sound pressure transmitted through the plate by higher-order mechanical resonances, or by leakage of sound around the baffle.

Fig. 2B shows that the velocity underwent a $\sim 180^\circ$ phase change at the peak frequency. This is as expected at a mechanical resonance, which occurs as the plate impedance transitions from stiffness-dominated to mass-dominated

behavior. The pressure on the far-side had a similar transition, underscoring the fact that the far-side pressure is produced by the motion of the plate. At frequencies below the peak, inward velocity (inward = toward the plate away from the speaker) led the speaker-side pressure by 90° . Displacement always lags velocity by 90° , so at frequencies below the resonance, inward displacement was \sim in phase with the speaker-side pressure, consistent with the stiffness-dominated impedance of the plate at those frequencies. (Note: because the far-side pressure was relatively small, the speaker-side pressure is approximately equal to the pressure difference across the plate that drives its motion, and a careful calculation of the pressure difference is only needed at frequencies very close to the resonant frequency.) At frequencies above the resonance, velocity lagged speaker-side pressure by 90° , thus at these frequencies, speaker-side pressure (approximately equal to the pressure difference across the plate, as reasoned just above) was in phase with plate acceleration.

The far-side pressure led velocity by $\sim 90^\circ$ throughout – far-side pressure was in phase with plate acceleration. Thus, the air on the far side presented a mass-dominated impedance, and while the resonant motion of the plate produced significant pressure on the far-side, most of this pressure was not related to acoustic *power* transfer across the plate. This is to be expected since the pressure was measured very close to the pressure source (the plate), where near-field pressure would be large.

DISCUSSION

We explored several simple acousto-mechanical systems in order to gain insight into the TM/air-space system of the mammalian ear. We started with a tube+plate and variations, which displayed a series of acoustical and mechanical resonances. The mechanical and acoustic resonances occurred at similar frequencies and were difficult to uncouple. Thus we added a baffled plate system to the study, with which we could explore mechanical resonances separately. The first-order mechanical resonance appeared robustly, with a large peak in the motion and far-side pressure. Because the first-order resonance is a uni-modal motion, it is closely related to a simple mechanical spring-mass resonance. At this resonance, the far-side pressure was large, and when considering the TM/air-space system, it is clear that substantial pressure would be produced within the middle ear space. At higher order mechanical resonances, the modeling results of Fig. 1C indicate that the pressure transmission to the far side is relatively small. This makes sense since higher order resonances are not uni-modal. In these resonances different portions of the plate move out of phase and thus even large motions would not produce large far-side pressure. Relating back to the TM/air-space system, higher order resonances would not be expected to produce large pressures in the ME cavity. These concepts will be explored further in a longer paper that is in preparation.

ACKNOWLEDGMENTS

This work was supported by the Spanish Ministry of Education, Culture and Sport; the University of Malaga, Spain; the NIDCD and the Emil Capita Foundation. Thanks to Mailing Wu and Polina Varavva for sensor construction.

REFERENCES

- de La Rochefoucauld O and Olson ES (2010) “A sum of simple and complex motions on the eardrum and manubrium in gerbil,” *Hearing Research* 263, 9 – 15.
- Fay JP, Puria S and Steele CR (2006) “The discordant eardrum,” *PNAS USA* 103, 19743-19748.
- Khanna SM, Koester CJ, Willemin JF, Dändliker R and Rosskothén H (1996) “A noninvasive optical system for the study of the function of inner ear in living animals,” *SPIE* 2732, 64-81.
- Olson ES (1998) “Observing middle and inner ear mechanics with novel intracochlear pressure sensors,” *J Acoust Soc Am* 103: 3445 – 3463.
- Parent P and Allen J (2004) “Wave model of the cat tympanic membrane,” *J Acoust Soc Am* 122: 918-931.
- Rabbitt RD (1990) “A hierarchy of examples illustrating the acoustic coupling of the eardrum,” *J Acoust Soc Am* 87: 2566-82.
- Rosowski JJ, Cheng JT, Ravicz ME, Hüllig N, Hernandez-Montes M, Harrington E, and Furlong C (2009) “Computer-assisted time-averaged holograms of the motion of the surface of the mammalian tympanic membrane with sound stimuli of 0.4–25 kHz,” *Hearing Research* 253, 83-96.
- Tonndorf J and Khanna SM (1972) “Tympanic-membrane vibrations in human cadaver ears by time-averaged holography,” *J Acoust Soc Am* 52, 1221–33.